



# Dissolution kinetics of solid fuels used in COREX gasifier and its influence factors

Run-sheng Xu<sup>1,2</sup> · Jian-liang Zhang<sup>2</sup> · Wei Wang<sup>1</sup> · Hai-bin Zuo<sup>3</sup> · Zheng-liang Xue<sup>1</sup> · Ming-ming Song<sup>1</sup>

Received: 18 January 2017 / Revised: 19 April 2017 / Accepted: 21 April 2017 / Published online: 27 February 2018  
© China Iron and Steel Research Institute Group 2018

## Abstract

Carbon dissolution from solid fuels used in a COREX gasifier was investigated in a high-temperature furnace to investigate the influences of temperature, carbon structure and ash properties of solid fuels into molten iron on carbon dissolution behavior. The results showed that the final carbon content of molten iron and dissolution reaction rate of carbon increased as the temperature increased. However, the dissolution behavior of different solid fuels varied with their properties. At the same temperature, the dissolution reaction rate of solid fuel from high to low was coke, semi-coke and lump coal. The apparent reaction rate constants of solid fuel were calculated using the piecewise fitting method based on the experimental data. The analyzed results showed that the dissolution rates of solid fuels had a good correlation with their microcrystalline structures. Moreover, the carbon crystallite structures of solid fuels used in COREX had greater influence on dissolution behavior than their ash properties.

**Keywords** Solid fuel · COREX · Dissolution behavior · Temperature · Carbon structure · Ash property

## 1 Introduction

The COREX process is the first commercial new iron-making technology, which has been successfully applied in South Africa, South Korea, India and China [1–5]. Since the COREX3000 was relocated to Xinjiang province of China, Baosteel had made an adjustment to the fuels utilization for COREX, aiming to reduce the production cost through using the local cheap coal and coke resource. The practice in Baosteel COREX process in Xinjiang province has shown that not only many self-produced cokes but also

abundant lump coals and semi-cokes can be used as the gasifier's fuels [6–8]. However, the production practice of COREX3000 in Shanghai has found that the strength of coal char generated from the lump coal is less than that of coke. Furthermore, the size of coal char is less than 10 mm in the gasifier's hearth, resulting in the decrease in the liquid permeability of stock column [9–11]. If the small fuel particles are easily dissolved into the molten iron when the molten iron passes through the stock column, it greatly benefits to the improvement in the liquid permeability of stock column. However, the dissolution behavior of solid fuels depends on their intrinsic properties and the molten iron properties.

The factors governing carbonaceous materials dissolution in molten iron have been investigated in previous studies. McCarthy et al. [12] investigated the influence of ash on interfacial reactions between coke and liquid iron at 1550 °C using the sessile drop method. The results showed that reduction reactions of iron oxide and silica significantly occurred at the interface, limiting the accumulation of solute carbon. Silica had the greatest effect on the carbon dissolution due to its high content in coke ash. Wu and Sahaiwalla [13, 14] investigated the influence of the carbon structure, the carbon content and the sulfur content in

✉ Run-sheng Xu  
xu\_runsheng@163.com

✉ Wei Wang  
wangwei74@wust.edu.cn

<sup>1</sup> State Key Laboratory of Refractories and Metallurgy, Wuhan University of Science and Technology, Wuhan 430081, Hubei, China

<sup>2</sup> School of Metallurgical and Ecological Engineering, University of Science and Technology Beijing, Beijing 100083, China

<sup>3</sup> State Key Laboratory of Advanced Metallurgy, University of Science and Technology Beijing, Beijing 100083, China

initial molten iron on coal dissolution and found that the crystallite structure of coal had a significant effect on the carbon dissolution from coals. What's more, the carbon and sulfur in initial molten iron retarded the dissolution rate of carbon from coal more significantly than from graphite. Wright et al. [15, 16] established the kinetic model of graphite and coke dissolution in gas-stirred iron/carbon melts. Sun [17] developed a kinetic model for carbon dissolution; his study showed that the dissolution rate of carbon at high temperature was faster than that at low temperature, and the mass transfer in the liquid iron was the major limiting step for the carbon dissolution. Cham et al. [18, 19] measured the dissolution rate of carbon from two cokes prepared from Australian coals and synthetic graphite into liquid iron in the temperature range of 1450–1550 °C. The results demonstrated that the difference of dissolution rate of these solid fuels was attributed to mineral matter limiting the interfacial contact area between the carbon matrix and liquid iron. Gudenau et al. [20] and Khanna et al. [21] also considered that the behavior of ash at the reaction interface could strongly affect the dissolution rate. Jang et al. [22] revealed that temperature was one of the important factors that determined the dissolution rate. Dissolution rate of carbon and sulfur from cokes into molten iron increased with increasing temperature. In addition, they thought that sulfur dissolution did not affect the carbon dissolution rate in molten iron. Although the dissolution behavior of coke and coal used in blast furnace has been in detail investigated, the report on the dissolution behavior of solid fuels (lump coal, semi-coke, coke) used in COREX gasifier is limited. Therefore, the dissolution characters of different solid fuels cannot be determined.

In this paper, carbon dissolution from three solid fuels into molten iron at 1450, 1500 and 1550 °C was systematically studied. Carbon dissolution rate was calculated based on the kinetic model. The effects of temperature and solid fuel properties including carbon crystal structure, ash content and ash properties on carbon dissolution rate were also investigated, with an aim to reveal the influence factors of dissolution behavior of the solid fuels used in a COREX gasifier.

## 2 Experimental

### 2.1 Experimental material

Lump coal, coke and semi-coke were selected as the fuels to compare the difference of dissolution process of solid fuels used in the COREX. The proximate analysis and ultimate analysis are listed in Table 1.

### 2.2 Experimental apparatus and method

#### 2.2.1 Experimental apparatus

A high-temperature melting furnace (BLMT-1700 °C) made by Boleman Furnace Co., Ltd. was used for the test, as shown in Fig. 1. The heater of the furnace is an Si–Mo rod; the highest temperature of this furnace can reach 1700 °C, and the maximum heating rate is 15 °C/min. The furnace temperature is monitored by a type-B thermocouple. The chamber of the furnace is made by a high-purity alumina tube, whose outer diameter is 90 mm and inner diameter is 80 mm. The protection gas (pure Ar) is continuously purged from the bottom of the furnace and escaped from the upper.

The high-purity corundum crucible, with an outer diameter of 70 mm, an inner diameter of 60 mm and a height of 80 mm, was used to melt the iron–carbon powders. The

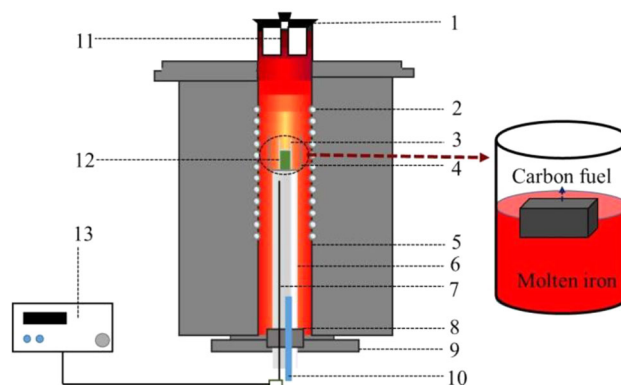


**Fig. 1** Diagram of high-temperature melting furnace. 1 Furnace cover; 2 heating element; 3 corundum tube; 4 corundum crucible; 5 protection crucible; 6 alumina hosting; 7 thermocouple; 8 alumina stopper; 9 furnace hosting; 10 protection gas import; 11 protection gas exit; 12 sample; 13 temperature control system

**Table 1** Proximate analysis and ultimate analysis of fuel samples (mass%)

Sample	Proximate analysis in air dry basis				Ultimate analysis in dry basis				
	Moisture	Volatile	Ash	Fixed carbon	C	H	O	N	St
Lump coal	1.89	23.26	2.64	72.21	80.90	4.04	10.06	1.05	0.26
Coke	0.19	1.46	11.42	86.93	85.33	0.17	0.01	1.00	0.81
Semi-coke	4.76	8.90	12.00	74.34	83.19	1.34	1.99	0.75	0.13

quartz glass tube was used to pick up iron liquid at the desired time during the fuel dissolution process.

### 2.2.2 Experimental process

The procedures of fuel dissolution experiment included fuel sample preparation, iron melting, carbon dissolution and iron sample testing. The detailed process is given below.

1. The large size fuels (lump coal, semi-coke and coke) were chosen and cut into cube samples and then dried in a drying oven at 40 °C for 2 h.
2. 400 g iron powder with 2% graphite powders was melted in the high-temperature furnace under Ar gas protection at the flow rate of 5 L/min. After the temperature reached the setting value, the furnace would be held at that temperature for 15 min to maintain uniform ambient temperature. And then, the lumpy fuel sample (30 mm × 30 mm × 60 mm) was added directly to the top surface of liquid iron for the dissolution reaction for 3 h, as shown in Fig. 1.
3. Molten iron samples were picked up directly from the corundum crucible via a quartz tube at desired time intervals (2, 4, 8, 10, 20, 40, 60, 80, 120 and 160 min). Carbon contents of the metal samples were determined by infrared absorption spectroscopy. The experimental scheme of dissolution reaction and sample preparation is shown in Fig. 2.

## 3 Results and discussion

### 3.1 Dissolution behavior

#### 3.1.1 Effect of temperature on dissolution reaction

The dissolution behavior of lump coal, semi-coke and coke at 1450, 1500 and 1550 °C was compared to investigate the

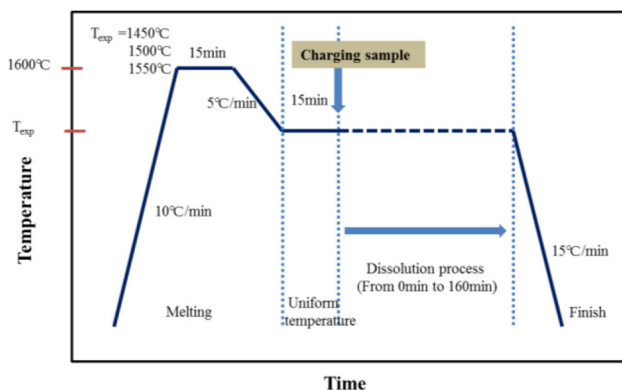


**Fig. 2** Experimental scheme of dissolution reaction and sample preparation

effects of temperature on the solubility and dissolution rate of different kinds of solid fuels used in the COREX gasifier. The carbon content in the molten iron at different reaction time is shown in Fig. 3.

It can be seen that the dissolution reaction of solid fuels used in the COREX gasifier can be divided into the quick dissolution stage (within 10 min) and the slow dissolution stage (10 min later). In addition, the carbon content curve moves to the upper right with increasing temperature, which indicates that the temperature has a great promotion on the dissolution of solid fuels. The maximum carbon content in the final reaction stage also increases with increasing temperature. The final carbon contents of the three fuels in molten iron after dissolution reaction are shown in Table 2. The theoretical saturated carbon content at different temperatures was also calculated by the following formula [23]:

$$w[C]_{\text{sat}} = 1.30 + 2.57 \times 10^{-3}T - 0.31w[\text{Si}] - 0.33w[\text{P}] - 0.45w[\text{S}] + 0.28w[\text{Mn}] \quad (1)$$

where  $w[C]_{\text{sat}}$  is the theoretical saturated carbon content in molten iron, %;  $T$  is the molten iron temperature, K; and  $w[\text{Si}]$ ,  $w[\text{P}]$ ,  $w[\text{S}]$  and  $w[\text{Mn}]$  are the Si, P, S and Mn contents in molten iron, respectively, %. Here, the Si, P, Mn and S contents in the molten iron were so small that their effect on the calculation was ignored. The calculated saturated carbon is also listed in Table 2. Compared the experimental final carbon content with the theoretical saturated carbon content, it can be found that the real saturated carbon content of the fuels used in the COREX gasifier is less than the calculated results at different temperatures. What's more, the real saturated carbon content of the fuels from less to more is lump coal, semi-coke and coke, which may be attributed to the microstructure and their composition of the fuels.

#### 3.1.2 Effect of fuel type on dissolution reaction

The difference of the dissolution behavior of three fuels at the same reaction temperature is shown in Fig. 4. It can be found that the change rule of carbon content curve of different fuels with the reaction time is the same, namely the carbon content first increases dramatically and then increases slowly. The dissolution rate of coke is faster than that of semi-coke, and the dissolution rate of lump coal is the lowest. The difference of dissolution rate of three fuels gradually reduces with increasing temperature. The above analysis revealed that the consumption rate of dead stock in the COREX hearth is determined by the fuel type, as well as the molten iron temperature.

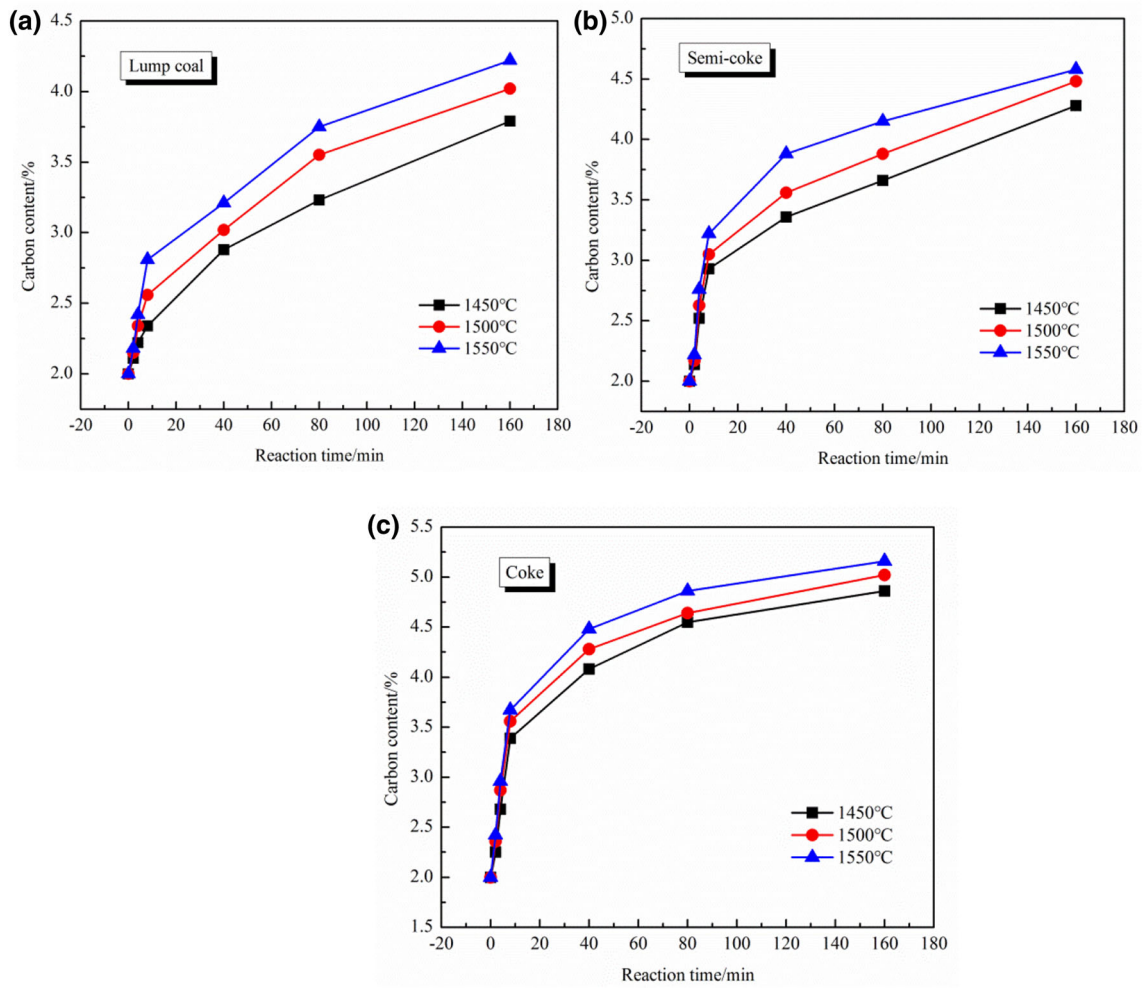


Fig. 3 Change of carbon content in molten iron as a function of time. a Lump coal; b semi-coke; c coke

Table 2 Final carbon content of different fuels in molten iron after reaction (wt%)

Fuel	1450 °C		1500 °C		1550 °C	
	Experimental value	Calculated value	Experimental value	Calculated value	Experimental value	Calculated value
Semi-coke	4.28	5.03	4.48	5.16	4.58	5.28
Lump coal	3.79	5.03	4.02	5.16	4.22	5.28
Coke	4.86	5.03	5.02	5.16	5.16	5.28

### 3.2 Kinetic analysis of dissolution of solid fuels used in COREX

#### 3.2.1 Kinetic model

Scholars [15, 18, 19] have revealed that the carbon dissolution process of coke can be divided into two stages: At the first stage, the dissolution reaction occurs at coke–melt interface, and the carbon atoms will be dissociated from the carbon matrix; at the second stage, the carbon diffusion

(mass transfer) takes place from the interface into molten iron. Orsten and Oeters [24] investigated the dissolution process of graphite column by the rotating cylinder method and showed that the dissolution rate of graphite column increased with increasing the rotating rate; thus, they proposed that the dissolution rate of graphite was controlled by the diffusion rate of graphite from interface to the molten iron. For the cube sample used in this experiment, a first-order kinetic equation was applied with assuming that the carbon dissolution was controlled by mass transfer.

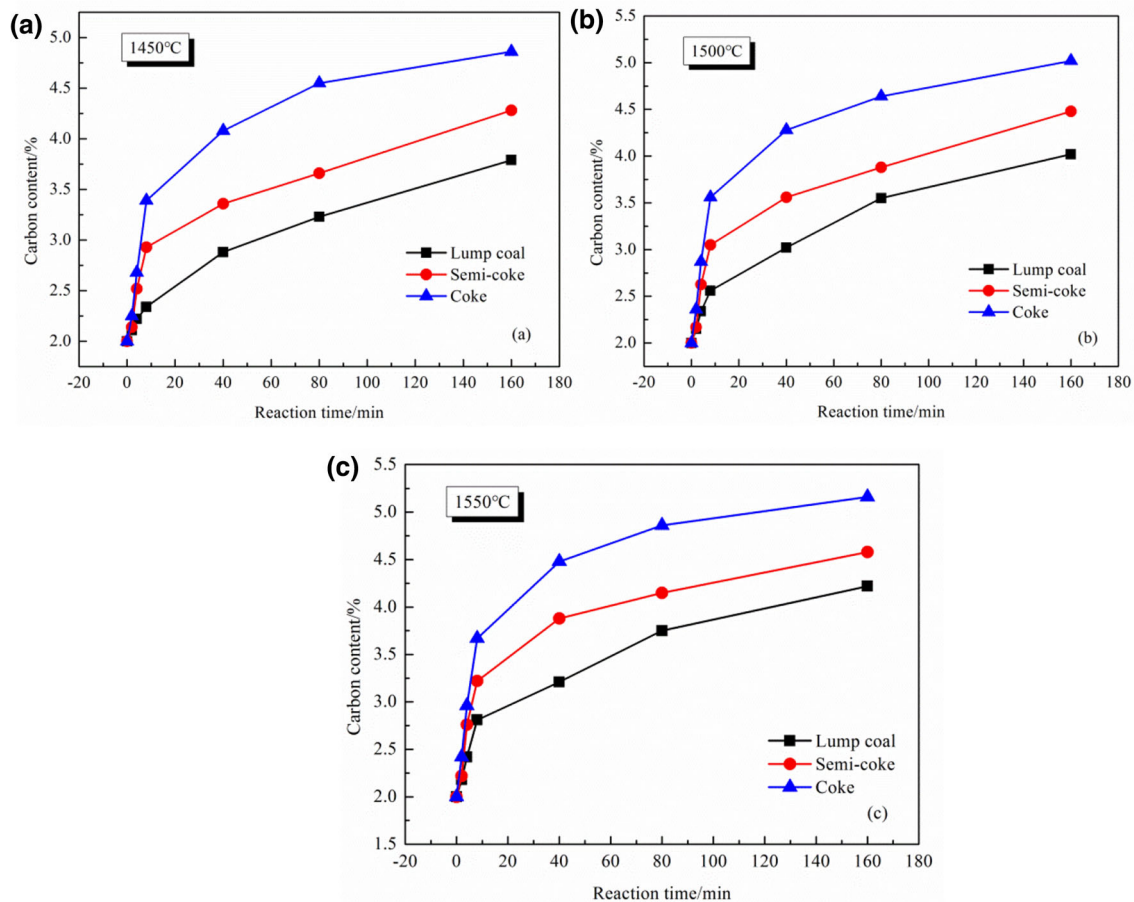


**Fig. 4** Variation of carbon content of molten iron. **a** At 1450 °C; **b** at 1500 °C; **c** at 1550 °C

$$V \frac{dC}{dt} = Ak_m(C_s - C_t) \quad (2)$$

where  $V$  is the volume of the molten iron bath,  $m^3$ ;  $A$  is the contract area between the fuel sample and the molten iron,  $m^2$ ;  $k_m$  is the mass transfer coefficient, (m/s);  $C_s$  is the final saturated carbon content, %; and  $C_t$  is the carbon content at reaction time  $t$ , %.

It was assumed that  $V$ ,  $A$  and  $k_m$  did not change during the reaction in this experiment, and then Eq. (3) could be obtained through the integration of Eq. (2).

$$\frac{V}{A} \ln \left( \frac{C_s - C_0}{C_s - C_t} \right) = k_m t \quad (3)$$

where  $C_0$  is the initial carbon content before the experiment (%).

The apparent reaction rate constant  $K$  can be expressed as

$$K = k_m \frac{A}{V} \quad (4)$$

The value of  $K$  can be obtained by the fitting slope of the curve of  $\ln[(C_s - C_0)/(C_s - C_t)]$  to  $t$ .

### 3.2.2 Kinetic analysis

The relationship between  $\ln[(C_s - C_t)/(C_s - C_0)]$  and  $t$  for the three fuels during the dissolution process is shown in Fig. 5. It can be observed that the curves can be divided into two parts with the reaction time of 8 min. The curve slope of the first part (less than 8 min) is higher than that of the second part (above 8 min). In studies of carbon dissolution in molten iron performed by Khanna et al. [21] and Chapman [25], similar trends were identified in dissolution data and the data were also divided into two periods. Applying such an approach to the data in this study, the piecewise fitting method was used to calculate the kinetic parameters. The fitting processes of the dissolution data of solid fuels through linear fitting method are shown in Fig. 6.

The curve slope can be obtained based on the fitting results, namely the apparent reaction rate constant of different solid fuels under different conditions can be obtained, as shown in Table 3.

The apparent reaction rate constant increases with increasing temperature. Moreover, the temperature has



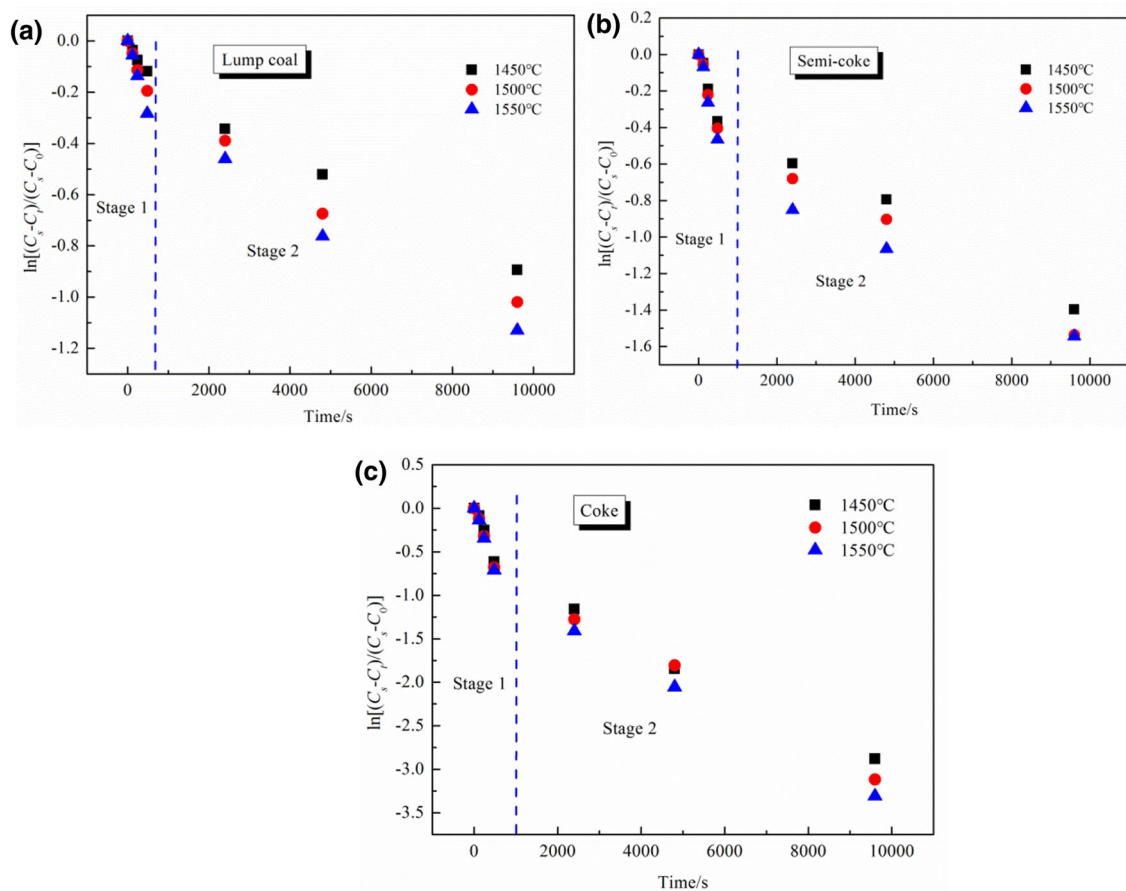


**Fig. 5** Relationship between  $\ln[(C_s - C_t)/(C_s - C_0)]$  and  $t$  for solid fuels. **a** Lump coal; **b** semi-coke; **c** coke

greater effect on the first dissolution stage than the second dissolution stage. The apparent reaction rate constant of lump coal has nearly tripled (increasing from  $2.63 \times 10^{-4}$  to  $5.81 \times 10^{-4}$  m/s) at the first dissolution stage, when the reaction temperature ranges from 1450 to 1550 °C. However, the effect degree of temperature on the dissolution rate varies with the fuel type. From the calculated results, the temperature has less influence on the dissolution rate of coke than those of the other two solid fuels. The apparent reaction rate constant of coke increases from  $1.21 \times 10^{-3}$  to  $1.46 \times 10^{-3}$  m/s when the temperature increases from 1450 to 1550 °C at the first dissolution stage. What's more, the change degree of dissolution rate of coke at the second stage is less than that at the first stage. It can also be indicated that, from Table 3, the apparent reaction rate constant of carbon fuels under the same condition from high to low is coke, semi-coke and lump coal. Therefore, the ability of molten iron to clear char powder in dead stock column is limited. Then, the following study was focused on the influence factors which led to the different dissolution rates among those solid fuels.

### 3.3 Effect of intrinsic properties of solid fuel on dissolution behavior

#### 3.3.1 Carbon crystallite structure

Carbon structures in coal contribute to the scattered X-ray intensities, as shown in Fig. 7 [26]. The (002) band at around  $26^\circ$  is generally considered as the average stack height of the aromatic planes of carbon crystallite, while (100) band at around  $44^\circ$  and (110) band at around  $81^\circ$  are generally considered as hexagonal structures [27–31]. According to the Scherrer equation [26], the structure parameters, such as interlayer spacing of the crystalline structure ( $d_{002}$ ), crystallite sizes ( $L_a$ ,  $L_c$ ) and layer number ( $n$ ), can be calculated. The analytical results of the carbon crystallite structure parameters of three fuels are listed in Table 4.

It can be found from Table 4 that the values of  $L_c$  and  $L_a$  from high to low are corresponding to lump coal, semi-coke and coke. It indicates that the ordered degree of carbon in lump coal, semi-coke and coke increases in turn. In order to investigate the relationship between carbon

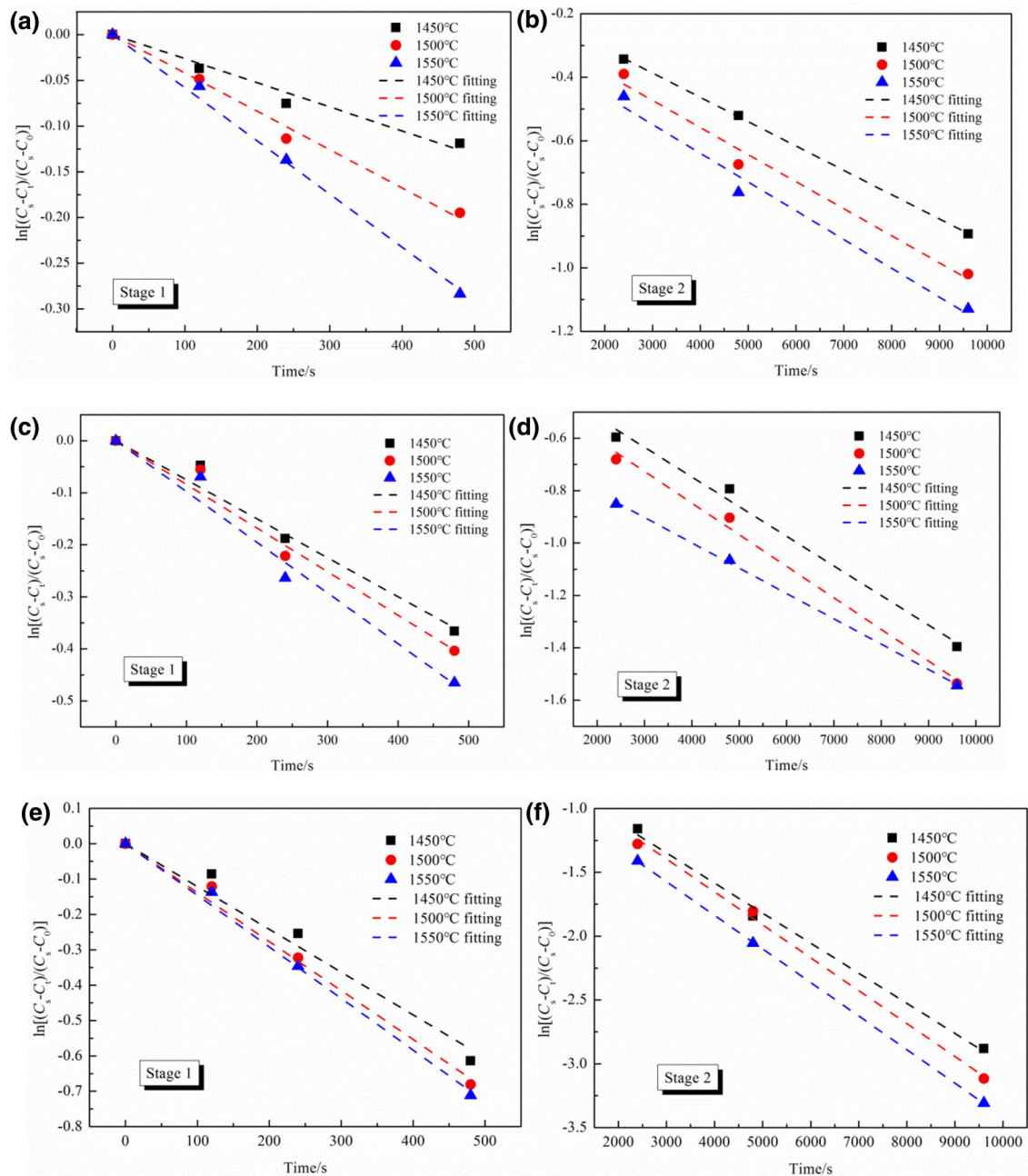


**Fig. 6** Fitting process of dissolution data of lump coal (a, b), semi-coke (c, d) and coke (e, f)

**Table 3** Apparent reaction rate constant under different conditions (m/s)

Fuels	Stage	1450 °C	1500 °C	1550 °C
Lump coal	Stage 1	$2.63 \times 10^{-4}$	$4.19 \times 10^{-4}$	$5.81 \times 10^{-4}$
	Stage 2	$7.66 \times 10^{-5}$	$8.52 \times 10^{-5}$	$9.06 \times 10^{-5}$
Semi-coke	Stage 1	$7.49 \times 10^{-4}$	$8.39 \times 10^{-4}$	$9.75 \times 10^{-4}$
	Stage 2	$1.13 \times 10^{-4}$	$1.21 \times 10^{-4}$	$0.97 \times 10^{-4}$
Coke	Stage 1	$1.21 \times 10^{-3}$	$1.38 \times 10^{-3}$	$1.46 \times 10^{-3}$
	Stage 2	$2.36 \times 10^{-4}$	$2.58 \times 10^{-4}$	$2.63 \times 10^{-4}$

crystallite structure of fuels and their dissolution behavior, the plot of apparent reaction rate against  $L_c$  value was obtained, as shown in Fig. 8. It can be found that the apparent reaction rate of dissolution increases with the increase in  $L_c$  value at the same reaction temperature. These results agree with the investigation results of Wu and Sahaiwalla [14]. The degree of difficulty of the carbon atom dissociation from a carbon matrix depends on the connection type among carbon atoms. The connection type of carbon atom in lump coal is in the form of 3-D net structure which is more complex than that in graphite.

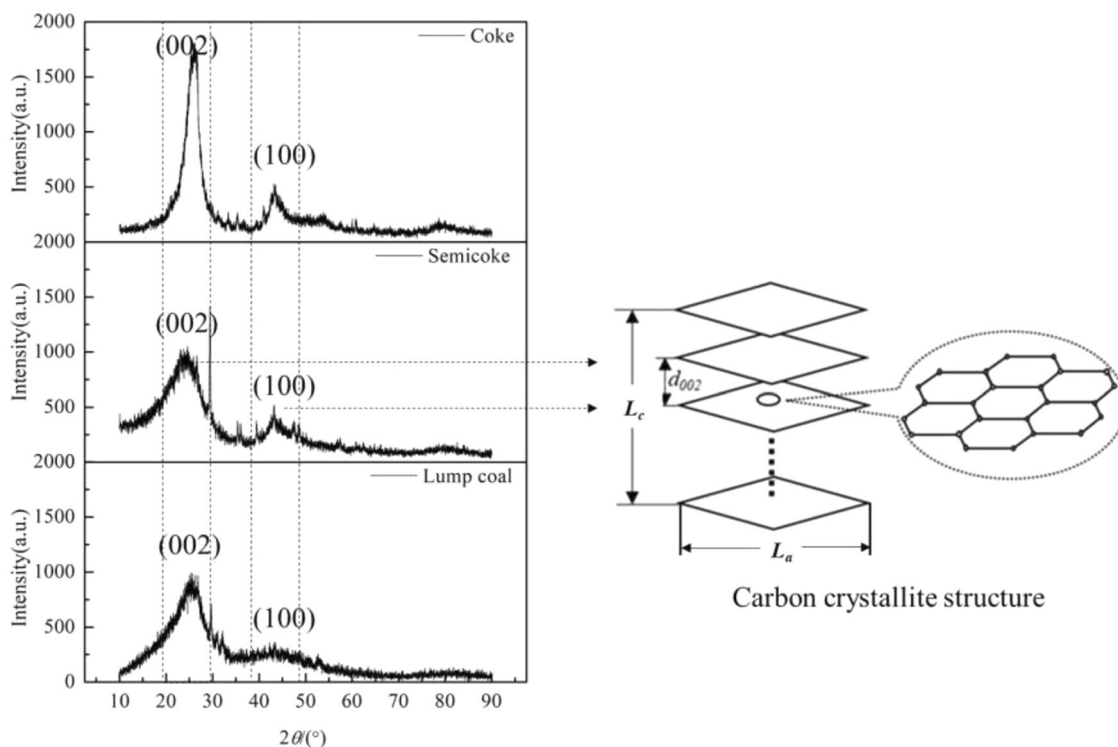


Fig. 7 X-ray diffraction curves of three fuels used in COREX

Table 4 Carbon crystallite structure parameters of three fuels

Fuel	$2\theta_{002}/(^{\circ})$	$2\theta_{100}/(^{\circ})$	$B_{002}/(^{\circ})$	$B_{100}/(^{\circ})$	$2\theta_{002}/(^{\circ})$	$L_a/nm$	$L_c/nm$	$d_{002}/nm$	$n$
Lump coal	24.58	41.58	10.37	17.23	24.58	1.01	0.78	0.36	2.14
Semi-coke	25.02	42.97	8.76	5.56	25.02	3.14	0.92	0.36	2.58
Coke	26.31	42.70	3.50	2.93	26.31	5.96	2.31	0.34	6.81

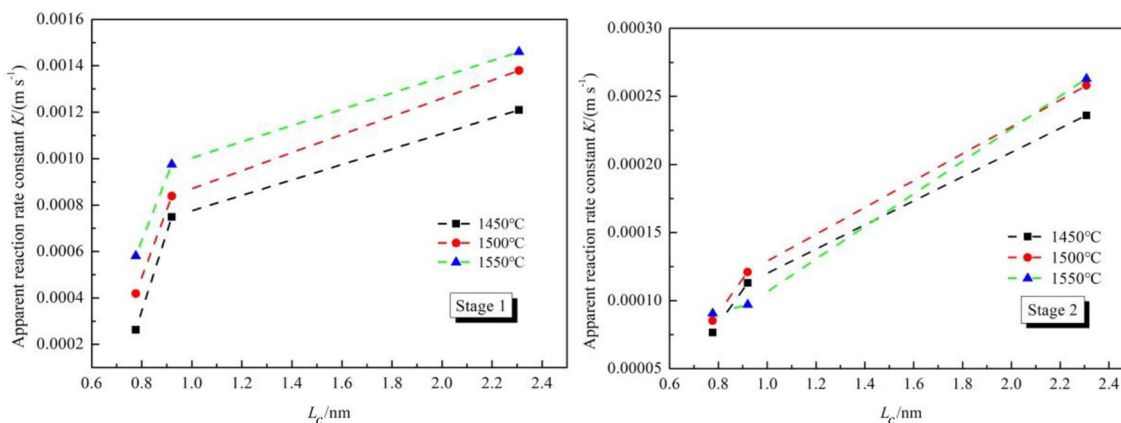
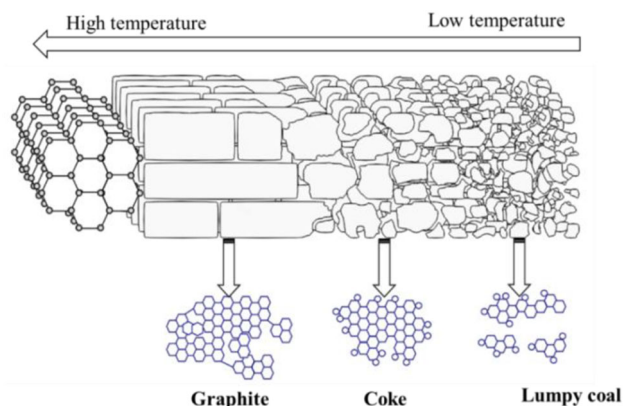


Fig. 8 Relationship between apparent reaction rate constant and  $L_c$

Therefore, the bond energy between atoms in lump coal is higher than that in graphite. It needs more energy to break down the C–C bond to complete the dissociation of carbon atom from lump coal than from the graphite.

The semi-coke is a product of the raw coal after coking at a moderate temperature (about 400–600 °C), while the coke is a product of the raw coal after coking at a high temperature (about 1000–1100 °C). With increasing the





**Fig. 9** Schematic model of change in lamellar structure of a graphitizing carbon with the increase in heat treatment temperature

heat treatment temperature, the random and disordered network connection structure gradually transforms into six-edge ring structure like graphite layer, as shown in Fig. 9 [32]. Therefore, the ordered degree of carbon structure in these fuels from high to low was ranked as coke, semi-coke and lump coal. The higher the ordered degree of carbon structure, the less the energy needed to dissociate the carbon atom from the crystal structure. Thus, the carbon dissolution rate gradually reduced with increasing the  $L_c$  value.

### 3.3.2 Ash properties

Ash is the mineral which is the other component except carbon in coal or coke. However, the composition, content and distribution of minerals in the carbon fuels vary with the solid fuels. Some researches [13, 17, 33] showed that the limited factors of coke dissolution process were the carbon atom dissociation process and the carbon atom transfer process at the reaction interface. Moreover, the carbon atom dissociation process was not only determined by the C–C bond connections type of carbon matrix, but also influenced by the properties of minerals. Therefore, the effect of ash on the dissolution reaction in molten iron was investigated.

### 3.4 Effect of ash content on carbon dissolution reaction

It can be found from Table 1 that the ash content in the raw fuels has a great difference, and the ash content in lump coal, semi-coke and coke is 2.64, 11.42 and 12.00%, respectively. When the sample was located into the molten iron, the volatile in the fuels was quickly devolatilized due to the high temperature. Based on this situation, the ratio of ash to carbon in fuels was more meaningful to study its influence on the dissolution reaction. The calculated results

of the ratio of ash to carbon show that the ratio of ash to carbon for lump coal is the least (3.66%), followed by the coke (13.14%), and the most one is semi-coke (16.14%). Commonly, the more ash in the fuel leads to the more inhibiting effect on the dissolution reaction. However, the dissolution reaction rate from high to low is coke, semi-coke and lump coal, which does not agree with the ash content order of solid fuels. The results reveal that the ash content in the fuels is not the key factor which influences the dissolution reaction rate.

### 3.5 Effect of ash composition on dissolution rate

As the carbon in solid fuels dissolves into the molten iron, the ash gradually appears, as shown in Fig. 10. Some minerals could become liquid slag, but some existed as solid slag and covered on the surface of carbon matrix. The solid slag could reduce the contact area between molten iron and carbon atom, while the properties of liquid slag would affect the transfer process of carbon atom, as shown in Fig. 10.

In order to evaluate the effect of ash composition on the dissolution reaction, the FactSage software was used in this study to investigate the properties of ash at high temperature. The ash compositions of fuels tested by the X-ray fluorescence (XRF) are shown in Table 5.

From Table 5, it can be found that the ash composition of three fuels is quite different. The sulfur content in coke and semi-coke is more than that in lump coal. The ash in lump coal contains much more CaO and Fe<sub>2</sub>O<sub>3</sub> as well as less SiO<sub>2</sub>, Al<sub>2</sub>O<sub>3</sub> and MgO compared with other fuels, while the ash in coke contains much more SiO<sub>2</sub> and Al<sub>2</sub>O<sub>3</sub> as well as less CaO, Fe<sub>2</sub>O<sub>3</sub> and MgO compared with others. The tested results reveal that the coal ash is alkaline, coke ash is acid, and semi-coke ash is neutral, which inevitably lead to the different properties of the ash at high temperature.

Table 6 lists the calculated results of the solid-phase content and liquid-phase content at the reaction interface. It can be found that the solid phase generated at the interface of semi-coke and iron is the least, while that at the interface of coke and iron is the most at the same temperature. It reveals that the reducing order of the ratio of solid phase to

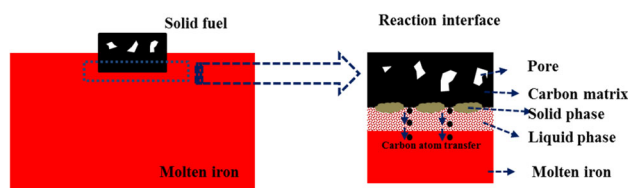


**Fig. 10** Ash transformation process during solid fuel dissolution

**Table 5** Ash composition of three solid fuels (wt%)

Fuel	SiO <sub>2</sub>	Al <sub>2</sub> O <sub>3</sub>	Fe <sub>2</sub> O <sub>3</sub>	CaO	MgO	TiO <sub>2</sub>	SO <sub>3</sub>	K <sub>2</sub> O	Na <sub>2</sub> O	MnO
Lump coal	13.67	5.7	27.42	32.23	4.46	0.49	13.68	0.08	0.95	0.36
Semi-coke	28.24	18.78	10.95	17.26	2.49	1.26	18.24	0.10	0.87	0.43
Coke	46.59	30.00	9.07	6.72	1.48	1.52	1.47	0.78	0.73	0.11

**Table 6** Calculated results of solid-phase content and liquid-phase content at reaction interface (wt%)

Temperature/°C	Lump coal		Semi-coke		Coke	
	Solid	Liquid	Solid	Liquid	Solid	Liquid
1450	16.00	84.00	5.91	94.09	16.35	83.65
1500	15.08	84.92	4.54	95.46	17.57	82.43
1550	14.14	85.86	3.60	96.40	27.51	72.49

liquid phase is from coke ash to lump coal ash and to semi-coke ash.

Moreover, the total amount of solid phase in the fuels which can be calculated according to the ash content and the solid-phase ratio will directly affect the carbon dissolution rate. The calculation equation was as follows:

$$m_s = W_1 \times W_2 / 100 \quad (5)$$

where  $m_s$  is the total amount of solid phase, %;  $W_1$  is the ash content in solid fuels except moisture and volatile, %; and  $W_2$  is the solid-phase ratio, %.

With increasing temperature, the total solid phase of lump coal and semi-coke at reaction interface decreases, while that of coke at the reaction interface increases, as shown in Table 7. It is suggested that some solid phase of lump coal and semi-coke at low temperature will melt and transform into liquid phase when the working temperature increases. However, some new solid phase can be generated through the reaction of liquid phase with carbon during the coke dissolution process.

From above theoretical analysis, it can be speculated that the more the solid phase on reaction surface is, the less the reaction contract areas are, and the higher the inhibition degree to carbon dissolution reaction is. However, the dissolution reaction rate of coke is the highest though it generates the maximum total amount of solid phase. This result reveals that the amount of solid phase at the reaction surface is not the main reason leading to the different dissolution reaction rates of three solid fuels.

In order to investigate the relationship between the properties of liquid phase and the dissolution reaction rate of different fuels, the main composition and the viscosity of liquid phase generated from ash at the reaction interface were calculated by FactSage software. The results are listed in Table 8.

**Table 7** Total solid phase in fuels at different temperatures

Fuel	Temperature/°C	W <sub>1</sub> /wt%	W <sub>2</sub> /wt%
Lump coal	1450	3.53	0.56
	1500	3.53	0.53
	1550	3.53	0.50
Semi-coke	1450	13.90	0.82
	1500	13.90	0.63
	1550	13.90	0.50
Coke	1450	11.61	1.90
	1500	11.61	2.04
	1550	11.61	3.19

It can be found from Table 8 that the viscosity of liquid phase at reaction interface of three fuels decreases with increasing temperature. The low viscosity of liquid phase benefits the transformation of carbon atom from reaction interface to molten iron. Therefore, the dissolution reaction would increase with increasing temperature of molten iron.

At the same temperature, the viscosity of liquid phase from low to high is ranked in order as lump coal, semi-coke and coke. And the viscosity of liquid phase generated by coke is much more than those generated by other fuels. The high viscosity of liquid phase generated by coke results from its special composition which contains above 80% acidic oxide (SiO<sub>2</sub> and Al<sub>2</sub>O<sub>3</sub>). These calculation results indicate that the viscosity property of generated liquid phase at the reaction interface of three fuels does not agree with their dissolution reaction rate. Namely, the dissolution reaction rate from high to low is coke, semi-coke and lump coal, while this rank order is just the opposite rank order of the viscosity of generated liquid phase. These results reveal that the viscosity property of liquid phase at the interface is not the main reason leading to the different dissolution reaction rates for these three fuels.

In conclusion, the microcrystal structure has the greatest effect on the dissolution reaction rate, which is the crucial factor to determine the fuel dissolution rate in this experiment. These results also agree with the findings of Wu and Sahaiwalla [14]. Therefore, in order to keep good permeability of stock column, it should try to reduce the generation of char powder in stock column.

**Table 8** Viscosity of liquid phase generated from ash under different conditions

Fuel	Temperature/°C	Composition of liquid phase/wt%				Viscosity/(Pa s)
		SiO <sub>2</sub>	Al <sub>2</sub> O <sub>3</sub>	CaO	MgO	
Lump coal	1450	28.30	11.53	51.26	8.26	0.22
	1500	27.95	11.47	51.52	8.37	0.17
	1550	27.70	11.43	51.99	8.16	0.13
Semi-coke	1450	44.91	28.36	22.67	3.35	5.82
	1500	43.44	28.44	24.08	3.35	3.27
	1550	41.38	28.95	25.57	3.43	1.84
Coke	1450	60.43	26.69	10.54	2.19	102.60
	1500	59.79	27.89	10.08	2.12	51.37
	1550	48.75	36.76	11.87	2.48	6.35

## 4 Conclusions

- High temperature could promote the dissolution reaction of solid fuels. With increasing temperature, both the final carbon content in molten iron and the dissolution rate could increase. At the same temperature, the dissolution rate of solid fuel from high to low was coke, semi-coke and lump coal. The difference of the dissolution behaviors of these three fuels reduced with increasing temperature, which indicated that the temperature rising could decrease the difference of dissolution caused by the fuel's intrinsic properties.
- The apparent reaction rate constants of three tested solid fuels were calculated using the piecewise fitting method based on the experimental data. The apparent reaction rate constant of solid fuels under the same condition from high to low was coke, semi-coke and lump coal. The results indicated that the ability of molten iron to clear char powder in dead stock column was limited. Therefore, in order to keep good permeability of stock column, it should try to reduce the generation of char powder in stock column.
- The dissolution rates of solid fuels had a good correlation with their microcrystalline structures. The increase in microcrystalline ordered degree ( $L_c$ ) of solid fuels could enhance the dissolution rate. However, there was no good corresponding relation between the ash properties and their dissolution behaviors. This study revealed that the carbon crystallite structure of solid fuels used in COREX had greater influence on dissolution behavior than their ash properties.

**Acknowledgements** The authors acknowledge the financial support from the National Natural Science Foundation of China (Nos. 51704216, 51474164 and U201760101) and China Postdoctoral Science Foundation (No. 2016M602378).

## References

- Z. Luo, H. Zhou, T. Zhang, Y. You, H. Li, Z. Zou, J. Iron Steel Res. Int. 22 (2015) 1098–1106.
- Z. Qiu, Z. Luo, H. Zhou, R. Chen, F. Wang, Z. Zou, J. Iron Steel Res. Int. 24 (2017) 18–26.
- H. Li, H. Zhou, T. Zhang, Y. You, Z. Zou, W. Xu, J. Iron Steel Res. Int. 23 (2016) 516–524.
- L. Han, Z. Luo, H. Zhou, Z. Zou, Y. Zhang, J. Iron Steel Res. Int. 22 (2015) 304–310.
- W. Shen, S. Wu, M. Kou, K. Du, Y. Sun, J. Iron Steel Res. Int. 22 (2015) 200–206.
- Z. Xue, Q. Zou, H. Xu, Xinjiang Steel 130 (2014) 1–4.
- R. Xu, J. Zhang, G. Wang, H. Zuo, Z. Liu, K. Jiao, Y. Liu, K. Li, Metall. Mater. Trans. B 47 (2016) 1–14.
- R. Xu, J. Zhang, G. Wang, H. Zuo, P. Li, H. Wang, H. Lin, S. Liu, J. Therm. Anal. Calorim. 123 (2015) 773–783.
- Y. Guo, W. Xu, J. Zhu, J. Zhang, Metall. Mater. Trans. B 44 (2013) 1078–1085.
- Y. Guo, W. Xu, J. Zhu, J. Zhang, Ironmak. Steelmak. 40 (2013) 545–550.
- F. Wang, C. Bai, Y. Yu, G. Qiu, S. Zhang, Ironmak. Steelmak. 36 (2009) 590–596.
- F. McCarthy, V. Sahajwalla, J. Hart, N. Saha-Chaudhury, Metall. Mater. Trans. B 34 (2003) 573–580.
- C. Wu, V. Sahajwalla, Metall. Mater. Trans. B 31 (2000) 243–251.
- C. Wu, V. Sahajwalla, Metall. Mater. Trans. B 31 (2000) 215–216.
- J.K. Wright, B.R. Baldock, Metall. Mater. Trans. B 19 (1988) 375–382.
- J.K. Wright, F. Taylo, ISIJ Int. 33 (1993) 529–538.
- H. Sun, ISIJ Int. 45 (2005) 1482–1488.
- S.T. Cham, R. Sakurovs, H. Sun, V. Sahajwalla, ISIJ Int. 46 (2006) 652–659.
- S.T. Cham, V. Sahajwalla, R. Sakurovs, H. Sun, M. Dubikova, ISIJ Int. 44 (2004) 1835–1841.
- H.W. Gudenau, J.P. Mulanza, D.G.R. Sharma, Steel Res. Int. 61 (1990) 97–104.
- R. Khanna, F. McCarthy, H. Sun, Metall. Mater. Trans. B 36 (2005) 719–729.
- D. Jang, Y. Kim, M. Shin, J. Lee, Metall. Mater. Trans. B 43 (2012) 1308–1314.
- F. Neumann, H. Schenck, W. Patterson, Giesserei 47 (1960) 709–716.

- [24] S. Orsten, F. Oeters, in: Proc. 5th Int. Steel Congress, Iron and Steel Society, Washington, 1986, pp. 143–155.
- [25] M. Chapman, Insoluble Oxide Product Formation and Its Effect on Coke Dissolution in Liquid Iron, University of Wollongong, Wollongong, 2009, 196–201.
- [26] L. Lu, V. Sahajwalla, C. Kong, D. Harris, Carbon 39 (2001) 1821–1833.
- [27] R. Xu, B. Dai, W. Wang, J. Schenk, Z. Xue, Fuel Process. Technol. 173 (2018) 11–20.
- [28] R. Xu, B. Dai, W. Wang, J. Schenk, A. Bhattacharyya, Z. Xue, Energ. Fuels (2017) <https://doi.org/10.1021/acs.energyfuels.7b03023>.
- [29] W. Wang, J. Wang, R. Xu, Y. Yu, Y. Jin, Z. Xue, Fuel Process. Technol. 159 (2017) 118–127.
- [30] W. Wang, B. Dai, R. Xu, J. Schenk, J. Wang, Z. Xue, Steel Res. Int. 88 (2017) e201700063.
- [31] O.O. Sonibare, T. Haeger, S.F. Foley, Energy 35 (2010) 5347–5353.
- [32] R. Taylor, Comprehensive Composite Materials 4 (2003) 387–426.
- [33] M.W. Chapman, B.J. Monaghan, Metall. Mater. Trans. B 39 (2008) 418–430.